

Comparison of Doubly Lithiated, Magnesiated, and Zincated Ferrocenes: $[\text{Fe}(\eta^5\text{-C}_5\text{H}_4)_2]_2\text{Zn}_2(\text{tmeda})_2$, the First Example of a [1.1]Ferrocenophane with Bridging First-Row Transition Metal Atoms

Alejandro Sánchez Perucha, Julia Heilmann-Brohl, Michael Bolte, Hans-Wolfram Lerner, and Matthias Wagner*

Institut für Anorganische und Analytische Chemie, Goethe-Universität Frankfurt, Max-von-Laue-Strasse 7, D-60438 Frankfurt (Main), Germany

Received August 8, 2008

Starting from doubly lithiated ferrocene $[\text{Fe}(\eta^5\text{-C}_5\text{H}_4)_2]_3\text{Li}_6(\text{tmeda})_2$ (**1**), the corresponding thf adduct $[\text{Fe}(\eta^5\text{-C}_5\text{H}_4)_2]_2\text{Li}_4(\text{thf})_6$ (**3**) was prepared by recrystallization of **1** from thf. In contrast to **1**, which features six Li^+ cations surrounded by 1,1'-ferrocenediyl fragments in a carousel arrangement, compound **3** contains only two ferrocenediyl anions bridged by four Li^+ cations. This comparison clearly reveals the strong impact of different supporting ligands on the solid-state structures of lithiated ferrocenes. The doubly magnesiated and zincated derivatives $[\text{Fe}(\eta^5\text{-C}_5\text{H}_4)_2]_3\text{Mg}_3(\text{tmeda})_2$ (**4**) and $[\text{Fe}(\eta^5\text{-C}_5\text{H}_4)_2]_2\text{Zn}_2(\text{tmeda})_2$ (**6**) were synthesized via salt metathesis using **1** and MgCl_2 or ZnCl_2 , respectively. Even though Mg^{2+} and Zn^{2+} are chemically related ions, the solid-state structures of **4** and **6** turned out to be distinctly different. Compound **4** possesses a cluster structure reminiscent of the lithiated aggregate **1**, whereas **6** represents the first example of a first-row transition metal-bridged [1.1]-ferrocenophane (*anti*-conformation). All three doubly metallated ferrocenes **3**, **4**, and **6** are suitable reagents for the preparation of 1,1'-disubstituted ferrocenes as has been exemplified for the synthesis of $\text{Fe}(\eta^5\text{-C}_5\text{H}_4\text{SiMe}_3)_2$ (**5**). We have also shown that **5** can be generated in yields exceeding 90% from $\text{Fe}(\eta^5\text{-C}_5\text{H}_4\text{Br})_2$, Me_3SiCl , and Rieke magnesium.

Introduction

Metallation of ferrocene is the entry point to a rich organo-metallic chemistry. Since the dilithiated precursor $[\text{Fe}(\eta^5\text{-C}_5\text{H}_4)_2]_3\text{Li}_6(\text{tmeda})_2$ (**1**; Scheme 1) was first reported in 1967,¹ it has been extensively used to synthesize a broad variety of functionalized ferrocenyl derivatives with applications ranging from homogeneous catalysis (e.g., planar-chiral ferrocene-based ligands)² to materials science (e.g., poly(ferrocenylene)s with useful optical, electronic and magnetic properties).³ High molecular weight poly(ferrocenylene)s were first reported by Manners et al. following the discovery of the ring-opening polymerization (ROP) of strained ring-tilted [1]ferrocenophanes.⁴

Triggered by this pioneering work, ample evidence has been gathered to show that the presence of the main group atoms B ,^{5–11} Si ,^{4,12–17} Ge ,^{18,19} P ,^{20–22} As ,²⁰ S ,^{23,24} or Se ²⁴ as bridging

elements in either *ansa*-ferrocenes or poly(ferrocenylene)s can confer new and interesting properties to the respective compound.

* To whom correspondence should be addressed. E-mail: Matthias.Wagner@chemie.uni-frankfurt.de. Fax: +49 69 798 29260.

(1) Rausch, M. D.; Ciappenelli, D. J. *J. Organomet. Chem.* **1967**, *10*, 127–136.

(2) Togni, A.; Hayashi, T., Eds. *Ferrocenes*; VCH: Weinheim, 1995.
(3) Manners, I. *Synthetic Metal-Containing Polymers*, Wiley-VCH: Weinheim, 2004.

(4) Foucher, D. A.; Tang, B.-Z.; Manners, I. *J. Am. Chem. Soc.* **1992**, *114*, 6246–6248.

(5) Braunschweig, H.; Dirk, R.; Müller, M.; Nguyen, P.; Resendes, R.; Gates, D. P.; Manners, I. *Angew. Chem., Int. Ed. Engl.* **1997**, *36*, 2338–2340.

(6) Fontani, M.; Peters, F.; Scherer, W.; Wachter, W.; Wagner, M.; Zanello, P. *Eur. J. Inorg. Chem.* **1998**, 1453–1465.

(7) Grosche, M.; Herdtweck, E.; Peters, F.; Wagner, M. *Organometallics* **1999**, *18*, 4669–4672.

(8) Berenbaum, A.; Braunschweig, H.; Dirk, R.; Englert, U.; Green, J. C.; Jäkle, F.; Lough, A. J.; Manners, I. *J. Am. Chem. Soc.* **2000**, *122*, 5765–5774.

(9) Scheibitz, M.; Heilmann, J. B.; Winter, R. F.; Bolte, M.; Bats, J. W.; Wagner, M. *Dalton Trans.* **2005**, 159–170.

(10) Heilmann, J. B.; Scheibitz, M.; Qin, Y.; Sundaraman, A.; Jäkle, F.; Kretz, T.; Bolte, M.; Lerner, H.-W.; Holthausen, M. C.; Wagner, M. *Angew. Chem., Int. Ed.* **2006**, *45*, 920–925.

(11) Heilmann, J. B.; Qin, Y.; Jäkle, F.; Lerner, H.-W.; Wagner, M. *Inorg. Chim. Acta* **2006**, *359*, 4802–4806.

(12) Osborne, A. G.; Whiteley, R. H. *J. Organomet. Chem.* **1975**, *101*, C27–C28.

(13) Rulkens, R.; Lough, A. J.; Manners, I. *J. Am. Chem. Soc.* **1994**, *116*, 797–798.

(14) Rulkens, R.; Lough, A. J.; Manners, I.; Lovelace, S. R.; Grant, C.; Geiger, W. E. *J. Am. Chem. Soc.* **1996**, *118*, 12683–12695.

(15) Nguyen, P.; Gómez-Elipe, P.; Manners, I. *Chem. Rev.* **1999**, *99*, 1515–1548.

(16) Manners, I. *Science* **2001**, *294*, 1664–1666.

(17) Bellas, V.; Rehahn, M. *Angew. Chem., Int. Ed.* **2007**, *46*, 5082–5104.

(18) Stoeckli-Evans, H.; Osborne, A. G.; Whiteley, R. H. *J. Organomet. Chem.* **1980**, *194*, 91–101.

(19) Foucher, D. A.; Edwards, M.; Burrow, R. A.; Lough, A. J.; Manners, I. *Organometallics* **1994**, *13*, 4959–4966.

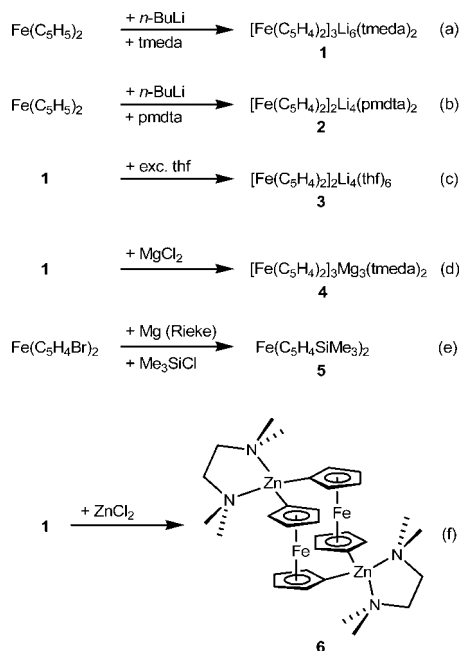
(20) Seyferth, D.; Withers, H. P., Jr. *Organometallics* **1982**, *1*, 1275–1282.

(21) Withers, H. P., Jr.; Seyferth, D.; Fellmann, J. D.; Garrou, P. E.; Martin, S. *Organometallics* **1982**, *1*, 1283–1288.

(22) Peckham, T. J.; Massey, J. A.; Honeyman, C. H.; Manners, I. *Macromolecules* **1999**, *32*, 2830–2837.

(23) Pudelski, J. K.; Gates, D. P.; Rulkens, R.; Lough, A. J.; Manners, I. *Angew. Chem., Int. Ed. Engl.* **1995**, *34*, 1506–1508.

(24) Rulkens, R.; Gates, D. P.; Balaishis, D.; Pudelski, J. K.; McIntosh, D. F.; Lough, A. J.; Manners, I. *J. Am. Chem. Soc.* **1997**, *119*, 10976–10986.

Scheme 1. Syntheses of Doubly Lithiated, Magnesiated, and Zincated Species 1–6^a


^a The chemical compositions of **1**–**4** refer to the results of X-ray crystal structure analyses. Reaction conditions: (a) Et₂O/hexane, r.t.; (b) hexane, r.t.; (c) thf, r.t.; (d) thf, r.t.; (e) thf, –30 °C to r.t.; (f) C₆H₆/thf, 0 °C to r.t.

Coming back to the original theme of metallated ferrocenes, the aforementioned results with *p*-block elements immediately raise the question how metal ions would behave as bridging units in [1]ferrocenophanes as well as in poly(ferrocenylene)s. Thus, the importance of metallated ferrocenes is not only restricted to their role as useful starting materials, but it is more and more recognized that these compounds, and especially their structural features, are interesting in their own right.²⁵

The main group metals Al,^{26,27} Ga,^{27,28} and Sn^{29,30} have already been introduced as bridging elements in [1]ferrocenophanes. Transition metal ions occupying the *ansa*-position are also known, either as constituents of discrete molecules (Ti,³¹ Zr,³¹ Hf,³¹ Ni,³² Pt³²) or as part of more elaborate cluster compounds (Mn,³³ Fe,³⁴ U³⁵).

The factors governing the formation of discrete metal-bridged [1]ferrocenophanes as opposed to [1.1]ferrocenophanes, poly-

mers or even cluster aggregates are still far from being understood. Steric influences together with the Lewis acidities of the metal ions appear to play an important role as has been shown for the reaction of [Fe(η^5 -C₅H₄)₂]₃Li₆(tmeda)₂ (**1**) with differently substituted aluminum halides: Treatment of **1** with (Pytsi)AlCl₂ [Pytsi = C(SiMe₃)₂SiMe₂(2-pyridyl)]²⁶ or (Me₂Ntsi)AlCl₂ [Me₂Ntsi = C(SiMe₃)₂(SiMe₂NMe₂)]²⁷ yielded the corresponding [1]ferrocenophanes. Here, intramolecular Al–N coordination in addition to steric shielding appears to be essential to obtain stable products. The similar reaction using less bulky and more Lewis acidic AlEt₂Cl formed a trinuclear aggregate in which three aluminum atoms are linked together by three 1,1'-ferrocenediyl subunits.³⁶ The structural motif of an [1]aluminaferrocenophane is absent in the latter complex, but a [1.1]dialuminaferrocenophane can be identified as substructure instead. An authentic example of a [1.1]ferrocenophane in which a base-stabilized aluminum ion is the bridging element was found upon treatment of [Fe(η^5 -C₅H₄)₂]₃Li₆(tmeda)₂ (**1**) with Cl₂Al(C₆H₄–CH₂NMe₂).³⁶

[1.1]Ferrocenophanes, which can be regarded as the cyclic analogs of poly(ferrocenylene)s, have been the subject of intense study³⁷ and examples with the elements B,³⁸ Si,^{39–42} P,⁴³ S⁴⁴ or the main group metals Al,^{36,45} Ga,^{45–48} In,⁴⁵ and Sn^{29,49} are known in the literature.

Moreover, a [1.1]dimercuroferrocenophane has been prepared and characterized in its Fe^{II}/Fe^{II}, Fe^{II}/Fe^{III}, and Fe^{III}/Fe^{III} states.⁵⁰ Surprisingly, however, the chemistry of transition metal-bridged [1.1]ferrocenophanes remains virtually unexplored to date.

Our group has a long-standing interest⁵¹ in *ansa*-ferrocenes,^{52–56} metallated ferrocenes^{34,57} as well as ferrocene-containing polymers^{6,7,9–11,58–63} and macrocycles.^{64–66} We have therefore embarked on a detailed study of the influence exerted by (i) different supporting ligands and (ii) the nature of the metal ions on the formation of [1]metallaferrocenophanes, [1.1]dimetallaferrocenophanes or ferrocene-containing cluster architectures. Herein, we describe our recent results regarding doubly lithiated,

(36) Braunschweig, H.; Burschka, C.; Clentsmith, G. K. B.; Kupfer, T.; Radacki, K. *Inorg. Chem.* **2005**, *44*, 4906–4908.

(37) Mueller-Westerhoff, U. T. *Angew. Chem., Int. Ed. Engl.* **1986**, *25*, 702–717.

(38) Scheibitz, M.; Winter, R. F.; Bolte, M.; Lerner, H.-W.; Wagner, M. *Angew. Chem., Int. Ed.* **2003**, *42*, 924–927.

(39) Park, J.; Seo, Y.; Cho, S.; Whang, D.; Kim, K.; Chang, T. J. *Organomet. Chem.* **1995**, *489*, 23–25.

(40) Zechel, D. L.; Foucher, D. A.; Pudelski, J. K.; Yap, G. P. A.; Rheingold, A. L.; Manners, I. J. *Chem. Soc., Dalton Trans.* **1995**, 1893–1899.

(41) Calleja, G.; Carré, F.; Cerveau, G.; Labbé, P.; Coche-Guérente, L. *Organometallics* **2001**, *20*, 4211–4215.

(42) Berenbaum, A.; Lough, A. J.; Manners, I. *Organometallics* **2002**, *21*, 4415–4424.

(43) Mizuta, T.; Imamura, Y.; Miyoshi, K.; Yorimitsu, H.; Oshima, K. *Organometallics* **2005**, *24*, 990–996.

(44) Ieong, N. S.; Chan, W. Y.; Lough, A. J.; Haddow, M. F.; Manners, I. *Chem.–Eur. J.* **2008**, *14*, 1253–1263.

(45) (a) Schachner, J. A.; Orłowski, G. A.; Quail, J. W.; Kraatz, H.-B.; Müller, J. *Inorg. Chem.* **2006**, *45*, 454–459. Note that Müller et al. have also published a crystal structure report on an Al(Cl)•tmeda-bridged [1.1]ferrocenophane: (b) Schachner, J. A.; Lund, C. L.; Quail, J. W.; Müller, J. *Acta Crystallogr.* **2005**, *E61*, m682–m684.

(46) Uhl, W.; Hahn, I.; Jantschak, A.; Spies, T. J. *Organomet. Chem.* **2001**, *637*–639, 300–303.

(47) Jutzi, P.; Lenze, N.; Neumann, B.; Stämmler, H.-G. *Angew. Chem., Int. Ed.* **2001**, *40*, 1424–1427.

(48) Althoff, A.; Jutzi, P.; Lenze, N.; Neumann, B.; Stämmler, A.; Stämmler, H.-G. *Organometallics* **2003**, *22*, 2766–2774.

(49) Clearfield, A.; Simmons, C. J.; Withers, H. P., Jr.; Seyferth, D. *Inorg. Chim. Acta* **1983**, *75*, 139–144.

(50) Kuz'mina, L. G.; Struchkov, Y. T.; Lemenovsky, D. A.; Urazowsky, I. F. *J. Organomet. Chem.* **1984**, *277*, 147–151.

(25) Venkatasubbaiah, K.; DiPasquale, A. G.; Bolte, M.; Rheingold, A. L.; Jäkle, F. *Angew. Chem., Int. Ed.* **2006**, *45*, 6838–6841.

(26) Schachner, J. A.; Lund, C. L.; Quail, J. W.; Müller, J. *Organometallics* **2005**, *24*, 785–787.

(27) Lund, C. L.; Schachner, J. A.; Quail, J. W.; Müller, J. *Organometallics* **2006**, *25*, 5817–5823.

(28) Schachner, J. A.; Lund, C. L.; Quail, J. W.; Müller, J. *Organometallics* **2005**, *24*, 4483–4488.

(29) Jäkle, F.; Rulkens, R.; Zech, G.; Foucher, D. A.; Lough, A. J.; Manners, I. *Chem.–Eur. J.* **1998**, *4*, 2117–2128.

(30) Sharma, H. K.; Cervantes-Lee, F.; Mahmoud, J. S.; Pannell, K. H. *Organometallics* **1999**, *18*, 399–403.

(31) Broussier, R.; Da Rold, A.; Gautheron, B.; Dromzee, Y.; Jeannin, Y. *Inorg. Chem.* **1990**, *29*, 1817–1822.

(32) Whittell, G. R.; Partridge, B. M.; Presly, O. C.; Adams, C. J.; Manners, I. *Angew. Chem., Int. Ed.* **2008**, *47*, 4354–4357.

(33) García-Alvarez, J.; Kennedy, A. R.; Klett, J.; Mulvey, R. E. *Angew. Chem., Int. Ed.* **2007**, *46*, 1105–1108.

(34) Sängler, I.; Heilmann, J. B.; Bolte, M.; Lerner, H.-W.; Wagner, M. *Chem. Commun.* **2006**, 2027–2029.

(35) Bucaille, A.; Le Borgne, T.; Ephritikhine, M.; Daran, J.-C. *Organometallics* **2000**, *19*, 4912–4914.

Table 1. Selected Crystallographic Data of the Compounds **3**(thf), **4**, and **6**(C₆H₆)₄

	3 (thf)	4	6 (C ₆ H ₆) ₄
formula	C ₄₄ H ₆₄ Fe ₂ Li ₄ O ₆ × C ₄ H ₈ O	C ₄₂ H ₅₆ Fe ₃ Mg ₃ N ₄	C ₃₂ H ₄₈ Fe ₂ N ₄ Zn ₂ × 4 C ₆ H ₆
fw	900.52	857.39	1043.62
color, shape	orange, block	orange, block	light brown, plate
temp (K)	173(2)	173(2)	173(2)
radiation	MoK α , 0.71073 Å	MoK α , 0.71073 Å	MoK α , 0.71073 Å
cryst syst	triclinic	monoclinic	monoclinic
space group	<i>P</i> 1	<i>C</i> 2/ <i>c</i>	<i>C</i> 2/ <i>c</i>
<i>a</i> (Å)	9.8205(9)	21.715(4)	31.401(2)
<i>b</i> (Å)	10.6036(9)	10.645(2)	18.6781(10)
<i>c</i> (Å)	11.7149(10)	17.523(4)	8.9302(6)
α (°)	74.735(7)	90	90
β (°)	80.070(7)	105.58(3)	90.241(6)
γ (°)	84.505(7)	90	90
<i>V</i> (Å ³)	1157.60(18)	3901.6(13)	5237.6(6)
<i>Z</i>	1	4	4
<i>D</i> _{calcd} (g cm ⁻³)	1.292	1.460	1.323
<i>F</i> (000)	480	1800	2192
μ (mm ⁻¹)	0.675	1.185	1.487
crystal size (mm ³)	0.52 × 0.48 × 0.45	0.25 × 0.24 × 0.15	0.27 × 0.24 × 0.13
no of rflns collected	22572	21655	28760
no of indep rflns (<i>R</i> _{int})	4365 (0.0465)	3643 (0.0462)	4928 (0.0777)
data/restraints/parameter	4365/0/289	3643/0/236	4928/0/289
GOOF on <i>F</i> ²	1.051	1.031	1.040
<i>R</i> 1, <i>wR</i> 2 (<i>I</i> > 2 σ (<i>I</i>))	0.0290, 0.0788	0.0283, 0.0658	0.0453, 0.1008
<i>R</i> 1, <i>wR</i> 2 (all data)	0.0315, 0.0799	0.0351, 0.0680	0.0695, 0.1091
Largest diff peak and hole (e Å ⁻³)	0.372, -0.390	0.494, -0.372	0.812, -0.629

magnesiates, and zincated ferrocenes, which represent useful organometallic reagents for further derivatizations.

Results and Discussion

X-ray crystal structure analyses of doubly lithiated ferrocene with *N,N,N',N'*-tetramethylethylenediamine (tmeda)⁶⁷ and *N,N,N',N',N''*-pentamethyldiethylenetriamine (pmdta)⁶⁸ as supporting ligands have already been published. We therefore decided to grow crystals of the corresponding thf adduct in order to

compare the solid-state structures as a function of varying donor additives. The Mg²⁺ cation and the Zn²⁺ cation have the same charges and ionic radii (*r*(Mg²⁺) = 0.71 Å, *r*(Zn²⁺) = 0.74 Å, coordination number = 4; *r*(Mg²⁺) = 0.86 Å, *r*(Zn²⁺) = 0.88 Å, coordination number = 6) and possess similar reactivities.⁶⁹ An analysis of the molecular structures of magnesiates and zincated ferrocenes will therefore reveal whether subtle differences in the properties of the metal ions can lead to significant changes in the molecular frameworks obtained.

Synthesis and Spectroscopy. The reaction of ferrocene with 2.5 equiv of *n*-BuLi in the presence of tmeda was reported in 1967 by Rausch et al. and leads to the selective monodeprotonation of each of the two cyclopentadienyl rings.¹ The resulting complex has the molecular formula [Fe(η^5 -C₅H₄)₂]₃Li₆(tmeda)₂ (**1**; Scheme 1).⁶⁷

Lithiation of ferrocene with *n*-BuLi in the presence of pmtda instead of tmeda was reported by Stucky et al. in 1978 and also leads to 1,1'-dilithiated ferrocene.⁶⁸ However, in this case the ratio between ferrocene and the supporting ligand is lower in the solid-state structure ([Fe(η^5 -C₅H₄)₂]₂Li₄(pmdta)₂, **2**; Scheme 1). The related thf adduct **3** was synthesized in good yields by recrystallization of **1** from a saturated thf solution at -30 °C. The ¹H NMR chemical shifts of the ferrocenediyl fragments of **3** (δ (¹H) = 3.58, 3.89) are very similar to those of **1** and the same is true for the ¹³C NMR signals. However, the quantitative replacement of tmeda for thf in the crystalline material is proven by the fact that signals for tmeda are missing and resonances of thf appear instead.

The preparation of doubly magnesiates ferrocene was carried out by salt metathesis. For this purpose, a thf solution of [Fe(η^5 -C₅H₄)₂]₃Li₆(tmeda)₂ (**1**) was carefully layered with MgCl₂ in thf at room temperature. Red crystals of [Fe(η^5 -C₅H₄)₂]₃Mg₃(tmeda)₂ (**4**; Scheme 1) grew at the interface over a period of 12 h (Scheme 1). The pyrophoric and extremely moisture-sensitive crystals were isolated in 66% yield. NMR spectra of **4** could not be recorded because the compound is insoluble in

(51) Ma, K.; Scheibitz, M.; Scholz, S.; Wagner, M. *J. Organomet. Chem.* **2002**, 652, 11–19.

(52) Jäkle, F.; Priermeier, T.; Wagner, M. *J. Chem. Soc., Chem. Commun.* **1995**, 1765–1766.

(53) Jäkle, F.; Mattner, M.; Priermeier, T.; Wagner, M. *J. Organomet. Chem.* **1995**, 502, 123–130.

(54) Herdtweck, E.; Jäkle, F.; Opromolla, G.; Spiegler, M.; Wagner, M.; Zanello, P. *Organometallics* **1996**, 15, 5524–5535.

(55) Jäkle, F.; Priermeier, T.; Wagner, M. *Organometallics* **1996**, 15, 2033–2040.

(56) Herdtweck, E.; Jäkle, F.; Wagner, M. *Organometallics* **1997**, 16, 4737–4745.

(57) Scholz, S.; Green, J. C.; Lerner, H.-W.; Bolte, M.; Wagner, M. *Chem. Commun.* **2002**, 36–37.

(58) Jäkle, F.; Priermeier, T.; Wagner, M. *Chem. Ber.* **1995**, 128, 1163–1169.

(59) Dinnebier, R. E.; Wagner, M.; Peters, F.; Shankland, K.; David, W. I. F. *Z. Anorg. Allg. Chem.* **2000**, 626, 1400–1405.

(60) Scheibitz, M.; Bats, J. W.; Bolte, M.; Lerner, H.-W.; Wagner, M. *Organometallics* **2004**, 23, 940–942.

(61) Haghiril Ilkhechi, A.; Scheibitz, M.; Bolte, M.; Lerner, H.-W.; Wagner, M. *Polyhedron* **2004**, 23, 2597–2604.

(62) Haghiril Ilkhechi, A.; Mercero, J. M.; Silanes, I.; Bolte, M.; Scheibitz, M.; Lerner, H.-W.; Ugalde, J. M.; Wagner, M. *J. Am. Chem. Soc.* **2005**, 127, 10656–10666.

(63) Wagner, M. *Angew. Chem., Int. Ed.* **2006**, 45, 5916–5918.

(64) Ding, L.; Fabrizi de Biani, F.; Bolte, M.; Zanello, P.; Wagner, M. *Organometallics* **2000**, 19, 5763–5768.

(65) Dinnebier, R. E.; Ding, L.; Ma, K.; Neumann, M. A.; Tanpipat, N.; Leusen, F. J. J.; Stephens, P. W.; Wagner, M. *Organometallics* **2001**, 20, 5642–5647.

(66) Ding, L.; Ma, K.; Dürner, G.; Bolte, M.; Fabrizi de Biani, F.; Zanello, P.; Wagner, M. *J. Chem. Soc., Dalton Trans.* **2002**, 1566–1573.

(67) Butler, I. R.; Cullen, W. R.; Ni, J.; Rettig, S. J. *Organometallics* **1985**, 4, 2196–2201.

(68) Walczak, M.; Walczak, K.; Mink, R.; Rausch, M. D.; Stucky, G. *J. Am. Chem. Soc.* **1978**, 100, 6382–6388.

(69) Holleman, A. F.; Wiberg, N. *Lehrbuch der Anorganischen Chemie*, 101 ed.; de Gruyter: Berlin, 1995.

all common inert solvents. Comparable species can also be prepared either via the Grignard reaction of 1,1'-dibromoferrrocene⁷⁰ with commercially available Mg turnings (which gives only moderate yields⁷¹) or via deprotonation of ferrocene with *n*-Bu₂Mg/*n*-BuLi/TMPH (which inevitably leads to contamination with lithium ions and 2,2,6,6-tetramethylpiperidine (TMP)⁷²). In the course of the present study we have found that 1,1'-disilylation of ferrocene (**5**; Scheme 1) proceeds with yields exceeding 90% when Rieke magnesium⁷³ is used in the Grignard reaction with 1,1'-dibromoferrrocene.⁷⁰

The lithiated species [Fe(η^5 -C₅H₄)₂)₃Li₆(tmeda)₂ (**1**) is also an excellent precursor for the formation of zincated ferrocenes. Upon mixing a slurry of **1** in C₆H₆ with a solution of 1 equiv of ZnCl₂ in a minimum amount of thf at 0 °C, an orange solid precipitated, which was subsequently extracted into C₆H₆. Storing the extract at 5 °C for two weeks yielded a crop of orange crystals which were identified by X-ray crystallography as the Zn-bridged [1.1]ferrocenophane **6** (Scheme 1, Figure 5). Compound **6** shows two pseudo triplets (4.49 ppm, 4.78 ppm) in the ¹H NMR spectrum and two carbon resonances at δ (¹³C) = 69.1 and 76.0. This signal pattern is not in accord with a rigid *anti*-conformation of **6** in solution (average C_{2h} symmetry) but can easily be explained by assuming a rapid degenerate *anti*-to-*anti* isomerization which results in an average D_{2h} symmetry of the molecular framework.

To test the suitability of **3**, **4**, and **6** as starting materials for the preparation of other 1,1'-disubstituted ferrocene derivatives, the compounds were treated with excess Me₃SiCl to prepare the known disilylated ferrocene Fe(η^5 -C₅H₄SiMe₃)₂ (**5**).⁷⁴ **5** was obtained in good yields of 80% (**3**), 70% (**4**; cf. 92% via the Grignard reaction with Rieke magnesium), and 85% (**6**).

X-ray Crystallography. X-ray crystallography on [Fe(η^5 -C₅H₄)₂)₃Li₆(tmeda)₂ (**1**) revealed a solid-state structure in which four lithium ions (Li(2), Li(2A), Li(3), Li(3A)) are surrounded by three 1,1'-ferrocenediyl subunits in a "carousel" arrangement (Figure 1).^{34,67} Two external lithium ions (Li(1), Li(1A)) adopt bridging positions between two ferrocenediyl fragments and are further bonded to tmeda ligands.

The molecule possesses a C₂ axis running through Fe(2). The bonding modes of Li(1) and Li(1A) resemble those expected for a hypothetical lithium-bridged [1.1]ferrocenophane, while the four internal lithium ions adopt the *ansa*-positions of [1]ferrocenophane substructures.

An X-ray crystal structure analysis of the pmdta-containing complex [Fe(η^5 -C₅H₄)₂)₂Li₄(pmdta)₂ (**2**) showed that the tridentate amine induces a remarkably different arrangement in the solid state (Figure 1).⁶⁸ Two rather than three 1,1'-ferrocenediyl subunits are present in an aggregate possessing inversion symmetry. The dimeric composition is held together by two three-coordinate lithium ions adopting *ansa*-positions (Li(2), Li(2A)). It has been suggested⁶⁷ that there is possibly an additional Li-Fe bond through the *e_g* orbitals of the iron

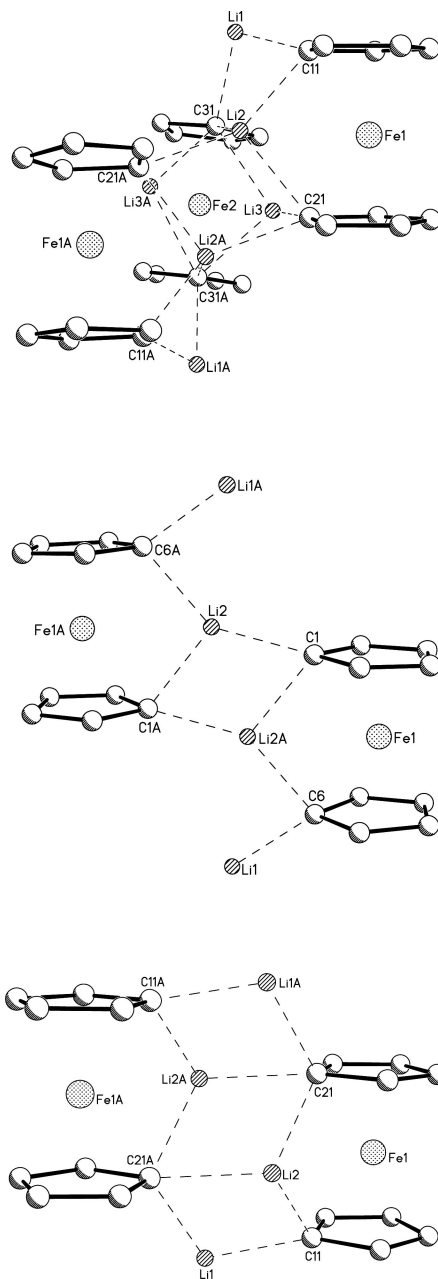


Figure 1. Comparison of the ferrocenediyl-Li⁺ cores of **1**³⁴ (top; η^2 -tmeda at Li(1) omitted), **2**⁶⁸ (middle; η^3 -pmdta at Li(1) omitted), and **3** (bottom; 2 thf ligands at Li(1) and 1 thf ligand at Li(2) omitted).

atom (Li(2)-Fe(1A) = 2.667(8) Å).⁷⁵ Two more lithium ions (Li(1), Li(1A)) are present in the structure of **2**, each of them wrapped by one pmdta ligand and thus forming only one short Li⁺-C₅H₄ contact. It is worth mentioning that the key structural features of [Fe(η^5 -C₅H₄)₂)₂Li₄(pmdta)₂ (**2**) are essentially identical with those of the related manganese complex [Mn(η^5 -C₅H₄)(η^6 -C₆H₅)₂)Li₄(pmdta)₂.⁷⁶

(70) Shafir, A.; Power, M. P.; Whitener, G. D.; Arnold, J. *Organometallics* **2000**, *19*, 3978–3982.

(71) Shechter, H.; Helling, J. F. *J. Org. Chem.* **1961**, *26*, 1034–1037.

(72) Henderson, K. W.; Kennedy, A. R.; Mulvey, R. E.; O'Hara, C. T.; Rowlings, R. B. *Chem. Commun.* **2001**, 1678–1679.

(73) Rieke, R. D.; Hanson, M. V. *Tetrahedron* **1997**, *53*, 1925–1956.

(74) Cunningham, A. F., Jr. *J. Am. Chem. Soc.* **1991**, *113*, 4864–4870.

(75) Ugalde et al. have studied the [ferrocene-Li]⁺ complex theoretically and located two minima on the energy surface. One of them has the Li⁺ ion bonded laterally to the iron atom at a distance of 2.4 Å. (cf. Irigoras, A.; Mercero, J. M.; Silanes, I.; Ugalde, J. M. *J. Am. Chem. Soc.* **2001**, *123*, 5040–5043) The [1.1]diborataferrocenophane reported by our group (cf. ref 38) proved to be a highly efficient lithium scavenger. One naked Li⁺ ion is located in the middle of the cavity with Li-Fe distances of 2.706(5) and 2.720(6) Å.

(76) Braunschweig, H.; Kupfer, T.; Radacki, K. *Angew. Chem., Int. Ed.* **2007**, *46*, 1630–1633.

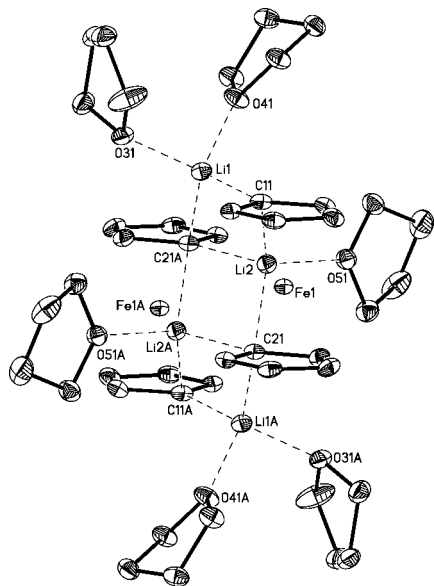


Figure 2. Structure of **3(thf)** in the crystal. Displacement ellipsoids drawn at the 50% probability level; hydrogen atoms and one molecule of noncoordinating thf omitted for clarity. Selected bond lengths (Å), atom...atom distances (Å), and bond angles (°): Li(1)–C(11) = 2.181(3), Li(1)–C(21A) = 2.252(3), Li(2)–C(11) = 2.213(3), Li(2)–C(21) = 2.280(3), Li(2)–C(21A) = 2.294(3), Li(1)···Li(2) = 2.469(4), Li(1)···Li(2A) = 3.530(4), Li(2)···Li(2A) = 2.458(5), Li(2)···Fe(1) = 2.726(3); C(11)–Li(1)–C(21A) = 113.0(1), C(11)–Li(2)–C(21) = 94.7(1), C(11)–Li(2)–C(21A) = 110.2(1), C(21)–Li(2)–C(21A) = 115.0(1). Symmetry transformation used to generate equivalent atoms: A = $-x + 1, -y + 1, -z + 1$.

The thf adduct **3** was obtained from a saturated thf solution and crystallizes together with one noncoordinating solvent molecule (**3(thf)**). The cluster **3** in **3(thf)** has the chemical composition $[\text{Fe}(\eta^5\text{-C}_5\text{H}_4)_2]_2\text{Li}_4(\text{thf})_6$ in the solid state and features lithium cations in two distinctly different coordination environments (Figures 1, 2).

Li(1) is stabilized by two ferrocenediyl subunits via η^1 -bonding to C(11) and C(21A). Two thf molecules are completing the distorted tetrahedral ligand sphere of this Li^+ center. Li(2), in contrast, binds to the 1,1'-positions of one ferrocenediyl subunit (C(11), C(21)) and to the deprotonated carbon atom of a second ferrocenediyl moiety (C21A). In this case, only one thf molecule is therefore required to achieve tetra-coordination. The basic arrangement of Li^+ cations and 1,1'-ferrocenediyl anions in $[\text{Fe}(\eta^5\text{-C}_5\text{H}_4)_2]_2\text{Li}_4(\text{thf})_6$ (**3**) notably differs from the previously described structure of $[\text{Fe}(\eta^5\text{-C}_5\text{H}_4)_2]_3\text{Li}_6(\text{tmeda})_2$ (**1**) resembling more the solid-state structure of $[\text{Fe}(\eta^5\text{-C}_5\text{H}_4)_2]_2\text{Li}_4(\text{pmdta})_2$ (**2**): we observe a C_i -symmetric dimer with two internal and two external lithium ions (Figure 2). A closer inspection, however, reveals significant differences also between the solid-state structures of **2** and **3** (Figure 1). For example, each of the external cations in **3** is bonded to *two* cyclopentadienyl ligands rather than to only one C_5H_4 ring (both bond lengths Li(1)–C(11) = 2.181(3) Å/Li(1)–C(21A) = 2.252(3) Å in **3** lie in the same range as the single Li–C contact in **2** (2.112(1) Å)). Moreover, the lithium ions (Li(2), Li(2A)) of **2** are located in the plane spanned by the iron centers (Fe(1), Fe(1A)) and the deprotonated carbon atoms (C(1), C(1A), C(6), C(6A)) of the fully eclipsed ferrocenediyl fragments. In **3**, however, Li(2) and Li(2A) deviate by 0.848 Å into opposite directions from the corresponding plane Fe(1)/Fe(1A)/C(11)/C(11A)/C(21)/C(21A). The reason lies in the fact that each of

these lithium ions is coordinated by one thf molecule which results in a distorted tetrahedral ligand environment as opposed to the trigonal-planar ligand spheres of the lithium ions in **2**. As to be expected, tetra-coordination of the internal lithium ions in **3** leads to an elongation of all three Li–C bonds (Li(2)–C(11) = 2.213(3) Å, Li(2)–C(21) = 2.280(3) Å, Li(2)–C(21A) = 2.294(3) Å). It is also revealing to compare the molecular framework of $[\text{Fe}(\eta^5\text{-C}_5\text{H}_4)_2]_2\text{Li}_4(\text{thf})_6$ (**3**) with those of the related dilithiated bisbenzenechromium complex $[\text{Cr}(\eta^6\text{-C}_6\text{H}_5)_2]_2\text{Li}_4(\text{thf})_6$ ⁷⁷ and trochrocene complex $[\text{Cr}(\eta^5\text{-C}_5\text{H}_4)(\eta^7\text{-C}_7\text{H}_6)]_2\text{Li}_4(\text{thf})_6$.⁷⁸ The key structural features of all three aggregates are very much alike, apart from the following differences: Upon going from $[\text{Fe}(\eta^5\text{-C}_5\text{H}_4)_2]_2\text{Li}_4(\text{thf})_6$ (**3**) to $[\text{Cr}(\eta^6\text{-C}_6\text{H}_5)_2]_2\text{Li}_4(\text{thf})_6$, one of the thf ligands that are coordinated to an internal lithium cation in **3** is moved to an external lithium cation in $[\text{Cr}(\eta^6\text{-C}_6\text{H}_5)_2]_2\text{Li}_4(\text{thf})_6$. If we go from **3** to $[\text{Cr}(\eta^5\text{-C}_5\text{H}_4)(\eta^7\text{-C}_7\text{H}_6)]_2\text{Li}_4(\text{thf})_6$, both internal thf ligands are moved to the external lithium cations. As a consequence, each of the resulting $[\text{Li}(\text{thf})_3]^+$ fragments establishes only one Li– C_5H_4 bond - pretty much like the $[\text{Li}(\text{pmdta})]^+$ cations in $[\text{Fe}(\eta^5\text{-C}_5\text{H}_4)_2]_2\text{Li}_4(\text{pmdta})_2$ (**2**). In summary, the structure of $[\text{Fe}(\eta^5\text{-C}_5\text{H}_4)_2]_2\text{Li}_4(\text{thf})_6$ (**3**) can be regarded as a combination of the structural motifs of [1]lithioferrocenophane (considering Li(2)/Li(2A)) and of macrocyclic [1.1]dilithioferrocenophane (considering Li(1) and Li(1A)).

X-ray diffraction studies on the magnesiated ferrocene **4** reveal a composition according to the formula $[\text{Fe}(\eta^5\text{-C}_5\text{H}_4)_2]_3\text{Mg}_3(\text{tmeda})_2$ (Figure 3).

The molecule consists of three eclipsed ferrocenediyl moieties surrounding one magnesium ion (Mg(2)). Two more magnesium ions (Mg(1), Mg(1A)) are located on the top and at the bottom of this aggregate and each of them is chelated by one tmeda ligand. The molecule possesses a C_2 axis running through Fe(1) and Mg(2) and conferring chirality to the cluster. The central Mg(2) ion is bonded to all three ferrocenediyl fragments in a distorted tetrahedral fashion. With regard to the Fe(1)-ferrocene it adopts an *ansa*-position (Mg(2)–C(11) = Mg(2)–C(11A) = 2.355(2) Å), whereas only a single terminal bond is established to each of the two other (symmetry-related) ferrocenediyl moieties (Mg(2)–C(31) = Mg(2)–C(31A) = 2.191(2) Å). The Mg(1) ion bridges the Fe(1)-ferrocene and the Fe(2)-ferrocene with bond lengths of Mg(1)–C(11) = 2.228(2) Å and Mg(1)–C(21) = 2.156(2) Å. The shortest contact to the third, Fe(2A)-containing ferrocene is substantially longer than these values (Mg(1)–C(31A) = 2.635(2) Å). From the inspection of the Mg–C bonds it is evident that they become continuously longer the more they are tilted out of the plane of their attached cyclopentadienyl ring. Thus, short Mg–C bonds appear to be associated with a high degree of σ -character. The molecular framework of $[\text{Fe}(\eta^5\text{-C}_5\text{H}_4)_2]_3\text{Mg}_3(\text{tmeda})_2$ (**4**) is reminiscent of the "carousel" structure of $[\text{Fe}(\eta^5\text{-C}_5\text{H}_4)_2]_3\text{Li}_6(\text{tmeda})_2$ (**1**) and strikingly similar to the only other example of a structurally characterized doubly magnesiated ferrocene, i. e. $[\text{Fe}(\eta^5\text{-C}_5\text{H}_4)_2]_3\text{Mg}_3\text{Li}_2(\text{TMP})_2(\text{pyridine})_2$ (Figure 4).

The latter compound has been prepared by Mulvey et al. via the deprotonation of ferrocene with a mixture of bases (*n*-Bu₂Mg/*n*-BuLi/TMPH) and crystallized from toluene in the presence of pyridine.⁷² The connectivity pattern of the $[\text{Fe}(\eta^5\text{-C}_5\text{H}_4)_2]_3\text{Mg}_3$ core in $[\text{Fe}(\eta^5\text{-C}_5\text{H}_4)_2]_3\text{Mg}_3\text{Li}_2(\text{TMP})_2(\text{pyridine})_2$ follows precisely that of our tmeda adduct $[\text{Fe}(\eta^5\text{-C}_5\text{H}_4)_2]_3\text{Mg}_3$.

(77) Braunschweig, H.; Kupfer, T. *Organometallics* **2007**, 26, 4634–4638.

(78) Braunschweig, H.; Kupfer, T.; Lutz, M.; Radacki, K. *J. Am. Chem. Soc.* **2007**, 129, 8893–8906.

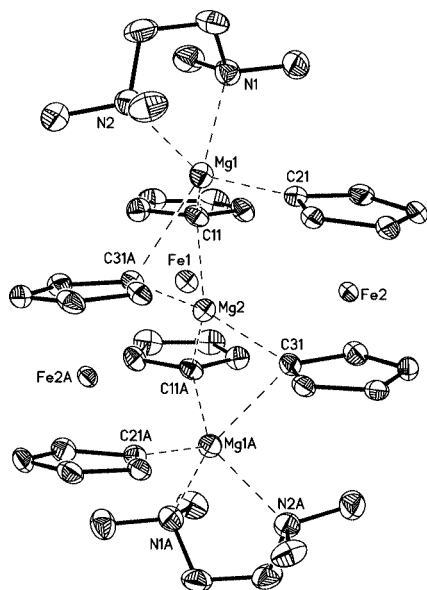


Figure 3. Structure of **4** in the crystal. Displacement ellipsoids drawn at the 50% probability level; hydrogen atoms omitted for clarity. Selected bond lengths (Å), atom...atom distances (Å), and bond angles (°): Mg(1)–C(11) = 2.228(2), Mg(1)–C(21) = 2.156(2), Mg(1)–C(31A) = 2.635(2), Mg(2)–C(11) = 2.355(2), Mg(2)–C(31) = 2.191(2), Mg(1)...Mg(2) = 2.851(1), Mg(2)...Fe(1) = 2.904(1), Mg(2)...Fe(2) = 3.426(1); C(11)–Mg(1)–C(21) = 113.7(1), C(11)–Mg(1)–C(31A) = 88.0(1), C(21)–Mg(1)–C(31A) = 98.1(1), C(11)–Mg(2)–C(11A) = 90.9(1), C(11)–Mg(2)–C(31) = 131.3(1), C(11)–Mg(2)–C(31A) = 96.4(1), C(31)–Mg(2)–C(31A) = 113.3(1), Mg(1)...Mg(2)...Mg(1A) = 170.2(1). Symmetry transformation used to generate equivalent atoms: A = $-x + 1, y, -z + 3/2$.

C₅H₄)₂]₃Mg₃(tmeda)₂ (**4**), even though the external magnesium ions Mg(1) and Mg(3) are only η^1 -coordinated by a bulky 2,2,6,6-tetramethylpiperidide ligand rather than η^2 -bonded to a tmeda molecule. For reasons of charge neutrality, [Fe(η^5 -C₅H₄)₂]₃Mg₃Li₂(TMP)₂(pyridine)₂ contains two [Li(pyridine)]⁺ complexes adopting bridging positions between TMP-nitrogen atoms and the adjacent cyclopentadienyl rings (Figure 4).

The zincated ferrocene [Fe(η^5 -C₅H₄)₂]₂Zn₂(tmeda)₂ (**6**) crystallizes from C₆H₆ with 4 equiv of solvent molecules (C₆H₆)₄. X-ray diffraction studies reveal a cyclic dimer which represents the first example of a [1.1]dimetallaferrocenophane with bridging first-row transition metal ions (Figure 5). The molecule adopts an *anti*-conformation similar to that of the Si-, Sn-, or In-bridged [1.1]ferrocenophanes mentioned above.

A crystallographic inversion center is located in the middle of the cage. The zinc atoms in **6**(C₆H₆)₄ lie at the center of a distorted [C₂N₂] tetrahedron formed by two C₅H₄ rings and one chelating molecule of tmeda (C(11)–Zn(1)–C(21A) = 126.6(1)°, N(1)–Zn(1)–N(2) = 81.0(1)°). The Zn–C bonds in **6**(C₆H₆)₄ (Zn(1)–C(11) = 1.990(3) Å, Zn(1)–C(21A) = 1.991(3) Å) are almost identical to those in the monozincated compound [Fe(η^5 -C₅H₄)₂]₂Zn(tmeda)⁷⁹ (Zn–C = 1.981(1) Å) and all four cyclopentadienyl rings are nearly coplanar to each other (dihedral angles: Cp(C(11)) // Cp(C(21)) = Cp(C(11)) // Cp(C(21A)) = 4.1°). These structural features suggest the macrocyclic framework of **6**(C₆H₆)₄ to be comparatively unstrained. According to empirical rules established by Miyoshi et al., the

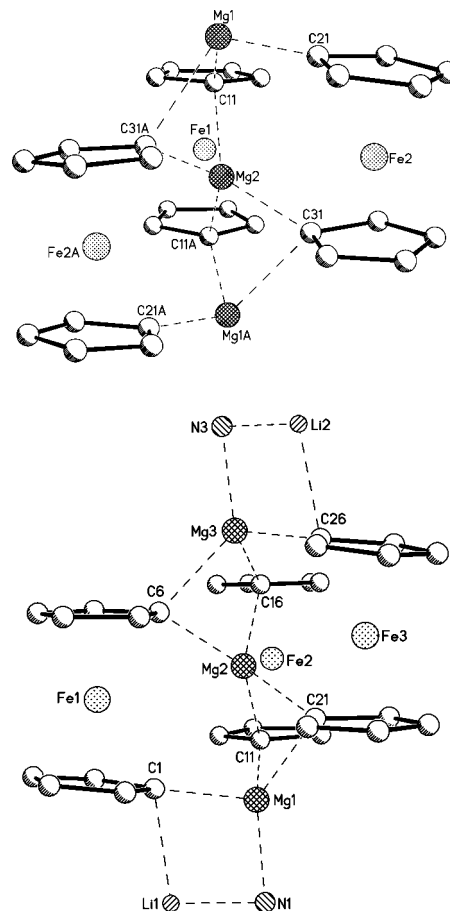


Figure 4. Comparison of the ferrocenediyl-Mg²⁺ cores of **4** (top; η^2 -tmeda at Mg(1) omitted) and [Fe(η^5 -C₅H₄)₂]₃Mg₃Li₂(TMP)₂(pyridine)₂ (bottom; pyridine at Li(1) and Li(2) omitted; only the nitrogen atoms N(1) and N(3) of the two TMP ligands shown).

anti-conformation is preferred for [1.1]ferrocenophanes [Fe(η^5 -C₅H₄)₂]₂(ER_x)₂ with (i) bulky substituents R at the bridgehead positions and (ii) C₅H₄–E bond lengths exceeding 1.85 Å.⁴³ Both conditions are met for **6**(C₆H₆)₄ such that its *anti*-conformation is in accord with a priori expectations. The distance between the Fe centers in **6**(C₆H₆)₄ (5.623 Å) is much smaller than in the analogous mercury-bridged [1.1]ferrocenophane (6.573 Å) but somewhat larger than in the Si- (5.170 Å),⁴⁰ Sn- (5.506 Å),⁴⁹ or In-bridged (5.724 Å)⁴⁵ derivatives.

Conclusion

The solid-state structures of doubly lithiated ferrocenes are greatly influenced by the nature of the supporting ligands as becomes evident from the X-ray crystallographical studies on [Fe(η^5 -C₅H₄)₂]₃Li₆(tmeda)₂ (**1**),⁶⁷ [Fe(η^5 -C₅H₄)₂]₂Li₄(pmdta)₂ (**2**),⁶⁸ and [Fe(η^5 -C₅H₄)₂]₂Li₄(thf)₆ (**3**).

A structural comparison of the magnesiated ferrocene [Fe(η^5 -C₅H₄)₂]₃Mg₃(tmeda)₂ (**4**; cluster compound) and the corresponding zincated derivative [Fe(η^5 -C₅H₄)₂]₂Zn₂(tmeda)₂ (**6**; [1.1]ferrocenophane) reveals that even subtle differences in the chemical properties of the metal ions have a pronounced effect on the molecular framework of metallated ferrocenes. The NMR spectra of **6** do not provide any indication for the presence of a second isomer in solution (e.g., a Zn-bridged [1]ferrocenophane). Moreover, the fact that samples of **6**(C₆H₆)₄ dissolve completely in C₆H₆ makes it highly unlikely that the [1.1]ferrocenophane establishes an equilibrium with the related Zn-bridged poly(ferrocenylene) structure in solution.

(79) Barley, H. R. L.; Clegg, W.; Dale, S. H.; Hevia, E.; Honeyman, G. W.; Kennedy, A. R.; Mulvey, R. E. *Angew. Chem., Int. Ed.* **2005**, *44*, 6018–6021.

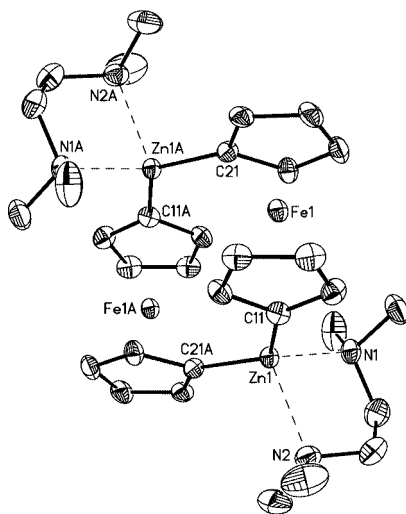


Figure 5. Structure of **6** in the crystal. Displacement ellipsoids drawn at the 50% probability level; hydrogen atoms and four molecules of C_6H_6 omitted for clarity. Selected bond lengths (Å), atom...atom distances (Å), and bond angles (°): Zn(1)–C(11) = 1.990(3), Zn(1)–C(21A) = 1.991(3), Zn(1)–N(1) = 2.210(3), Zn(1)–N(2) = 2.297(3), Zn(1)...Zn(1A) = 4.834(1), Fe(1)...Fe(1A) = 5.623(1); C(11)–Zn(1)–C(21A) = 126.6(1), N(1)–Zn(1)–N(2) = 81.0(1). Symmetry transformation used to generate equivalent atoms: $A = -x + 1/2, -y + 3/2, -z + 1$.

We are currently exploring the potential of **6** as starting material for the preparation of other 1,1'-disubstituted ferrocene derivatives. It has already turned out that one advantage of **6** is its solubility in the weakly coordinating and rather inert solvent C_6H_6 which enables us to perform transformations with highly electrophilic reagents under homogeneous conditions.

Experimental Section

General Remarks. All reactions were carried out under a nitrogen atmosphere using Schlenk tube techniques. Reaction solvents were freshly distilled under argon from Na/benzophenone (C_6H_6 , thf) prior to use; C_6D_6 and THF- d_8 were distilled under nitrogen from Na/benzophenone and stored in a Schlenk flask. NMR: Bruker AM 250, Avance 300, and Avance 400. Chemical shifts are referenced to residual solvent signals ($^1H/^{13}C\{^1H\}$: THF- d_8 : 3.58 ppm/67.7 ppm; C_6D_6 : 7.15 ppm/128.0 ppm). Abbreviations: vtr = virtual triplet, m = multiplet. NMR spectra were run at r. t. Trimethylsilylchloride (Me_3SiCl) was dried over CaH_2 and distilled under argon prior to use. $[Fe(\eta^5-C_5H_4)_2]_3Li_6(tmeda)_2$ (**1**),⁶⁷ $Fe(\eta^5-C_5H_4Br)_2$,⁷⁰ and Rieke magnesium⁷³ were synthesized according to literature procedures.

Synthesis of $[Fe(\eta^5-C_5H_4)_2]_2Li_4(thf)_6$ (3**).** **1** (0.15 g, 0.18 mmol/0.54 mmol ferrocenediyl units) was dissolved in thf (5 mL), the clear reddish solution was stirred for 2 h and then stored at $-30^\circ C$ overnight. Orange pyrophoric crystals of **3**(thf) precipitated after this time. The crystals were collected on a frit and dried under vacuum. Yield of **3**(thf): 0.20 g (0.22 mmol/0.44 mmol ferrocenediyl units; 80%). 1H NMR (300.0 MHz, THF- d_8): δ = 3.58 (vtr, 4H, C_5H_4), 3.89 (vtr, 4H, C_5H_4). ^{13}C NMR (75.5 MHz, THF- d_8): δ = 70.2 (C_5H_4), 71.3 (C_5H_4 -ipso), 79.9 (C_5H_4). The pyrophoric nature of **3**(thf) prevented satisfactory elemental analyses.

Synthesis of $[Fe(\eta^5-C_5H_4)_2]_3Mg_3(tmeda)_2$ (4**).** To $MgCl_2$ (0.20 g, 2.10 mmol) was added thf (10 mL) and the mixture was stirred at r. t. for 30 min. **1** (0.58 g, 0.70 mmol/2.10 mmol ferrocenediyl units) was dissolved in thf (10 mL) and the solution stirred at r. t. for 30 min. Stirring was stopped and the solution of **1** carefully layered with the solution of $MgCl_2$. Crystals of **4** grew at the interface at r. t. over a period of 12 h. They were isolated under

nitrogen and dried under vacuo. Yield of **4**: 0.39 g (0.46 mmol/1.38 mmol ferrocenediyl units; 66%). At r. t., compound **4** is insoluble in all common inert solvents; heating of a sample of **4** in THF- d_8 resulted in decomposition and ferrocene formation. Thus, no NMR data could be acquired. The pyrophoric nature of **4** prevented satisfactory elemental analyses. The doubly metallated nature of the bulk material was therefore confirmed by derivatization with Me_3SiCl (70% yield of $Fe(\eta^5-C_5H_4SiMe_3)_2$ (**5**)⁷⁴).

Synthesis of $[Fe(\eta^5-C_5H_4)_2]_2Zn_2(tmeda)_2$ (6**).** **1** (0.20 g, 0.24 mmol/0.72 mmol ferrocenediyl units) was suspended in C_6H_6 (10 mL) and the mixture was stirred for 30 min. $ZnCl_2$ (0.10 g, 0.73 mmol) in thf (3 mL) was added dropwise at $0^\circ C$. The mixture was stirred for 1 h at $0^\circ C$, allowed to reach r. t. and further stirred for 2 h. The orange solid precipitate obtained was extracted into hot C_6H_6 (2×5 mL). The combined extracts were concentrated to a volume of 3 mL and stored at $5^\circ C$. After two weeks, orange crystals of the highly air- and moisture-sensitive compound **6**(C_6H_6)₄ had grown, which were collected on a frit and dried under vacuum. Yield of **6**(C_6H_6)₄: 0.27 g (0.26 mmol/0.52 mmol ferrocenediyl units; 72%). 1H NMR (250.1 MHz, C_6D_6): δ = 2.01 (broad, 32H, CH_3 , CH_2), 4.49 (vtr, 8H, C_5H_4), 4.78 (vtr, 8H, C_5H_4). ^{13}C NMR (100.6 MHz, C_6D_6): δ = 46.8 (CH_3), 56.6 (CH_2), 69.1 (C_5H_4), 76.0 (C_5H_4). Anal. Calcd. for $C_{32}H_{48}Fe_2N_4Zn_2$ [731.18] \times 4 C_6H_6 [78.11]: C, 64.45; H, 6.95; N, 5.37. Found: C, 64.10; H, 6.85; N, 5.22.

Synthesis of $Fe(\eta^5-C_5H_4SiMe_3)_2$ (5**) from **3**(thf), **4** or **6**(C_6H_6)₄ and Me_3SiCl .** The doubly metallated ferrocene derivative was treated with thf (5 mL) and the solution (**3**(thf), **6**(C_6H_6)₄/slurry (**4**) was stirred at r. t. for 15 min. The mixture was cooled to $0^\circ C$ in an ice bath and Me_3SiCl in thf (3 mL) was added dropwise with stirring. The mixture was allowed to reach r. t. and further stirred for 1 h. A concentrated aqueous solution of $NaHCO_3$ (5 mL) was added and stirring was continued for 15 min. The crude mixture was extracted with $CHCl_3$ (3×5 mL) and the combined organic phases were dried over $MgSO_4$. After filtration, the solvent was removed from the filtrate under vacuo to give $Fe(\eta^5-C_5H_4SiMe_3)_2$ ⁷⁴ as an amber-colored oil which did not require further purification (NMR spectroscopical control).

Stoichiometries employed: (a) **3**(thf) (0.10 g, 0.11 mmol/0.22 mmol ferrocenediyl units), Me_3SiCl (0.07 mL, 0.06 g, 0.55 mmol), yield of **5**: 0.059 g (80%); (b) **4** (0.10 g, 0.12 mmol/0.36 mmol ferrocenediyl units), Me_3SiCl (0.12 mL, 0.10 g, 0.92 mmol), yield of **5**: 0.080 g (70%); (c) **6**(C_6H_6)₄ (0.10 g, 0.09 mmol/0.18 mmol ferrocenediyl units), Me_3SiCl (0.06 mL, 0.05 g, 0.45 mmol); yield of **5**: 0.054 g (85%).

Synthesis of $Fe(\eta^5-C_5H_4SiMe_3)_2$ (5**) with Rieke Magnesium.** $MgCl_2$ (0.37 g, 3.89 mmol) and K (0.27 g, 6.91 mmol) were refluxed in thf (15 mL) for 3 h to give a fine black dispersion of Rieke magnesium. The dispersion was cooled to $-30^\circ C$ and a thf (10 mL) solution of $Fe(\eta^5-C_5H_4Br)_2$ (0.30 g, 0.87 mmol) and Me_3SiCl (0.45 mL, 0.38 g, 3.51 mmol) was added dropwise during 15 min. The reaction mixture was allowed to warm to r. t. and further stirred for 3 h. Afterward, it was carefully quenched with a concentrated aqueous solution of $NaHCO_3$ (10 mL) and extracted with $CHCl_3$ (3×5 mL). The organic phases were combined and dried over $MgSO_4$. After filtration, the solvent was removed under vacuo to give $Fe(\eta^5-C_5H_4SiMe_3)_2$ (**5**).⁷⁴ Yield: 0.26 g (92%).

X-ray Crystal Structure Analysis of **3(thf), **4**, and **6**(C_6H_6)₄.** Data were collected on a STOE IPDS II two-circle diffractometer with graphite-monochromated Mo $K\alpha$ radiation. Empirical absorption corrections were performed using the MULABS⁸⁰ option in PLATON.⁸¹ The structures were solved by direct methods using the program SHELXS⁸² and refined against F^2 with full-matrix least-squares techniques using the program SHELXL-97.⁸³ **3** crystallizes together with 1 equiv of noncoordinated thf

(80) Blessing, R. H. *Acta Crystallogr.* **1995**, A51, 33–38.

(81) Spek, A. L. *J. Appl. Crystallogr.* **2003**, 36, 7–13.

(82) Sheldrick, G. M. *Acta Crystallogr.* **1990**, A46, 467–473.

which is disordered over two positions (**3**(thf); occupancy factors: 0.5, 0.5). **6** crystallizes together with 4 equiv of C_6H_6 (**6**(C_6H_6)₄). CCDC reference numbers: 296320 (**3**(thf)), 697369 (**4**), 697370 (**6**(C_6H_6)₄).

Acknowledgment. M.W. is grateful to the Deutsche Forschungsgemeinschaft (DFG) and the Fonds der Chemischen Industrie (FCI) for financial support.

Supporting Information Available: Crystallographic data of **3**(thf), **4**, and **6**(C_6H_6)₄ in the Crystallographic Information File format. This material is available free of charge via the Internet at <http://pubs.acs.org>.

OM800765A

(83) Sheldrick, G. M. *SHELXL-97, A Program for the Refinement of Crystal Structures*; Universität Göttingen: Göttingen, 1997.